and spread on the whole zeolite surface but there is coalescence, and depletion in different parts of zeolite, it leads to a decrease in the activity of active sights between them.

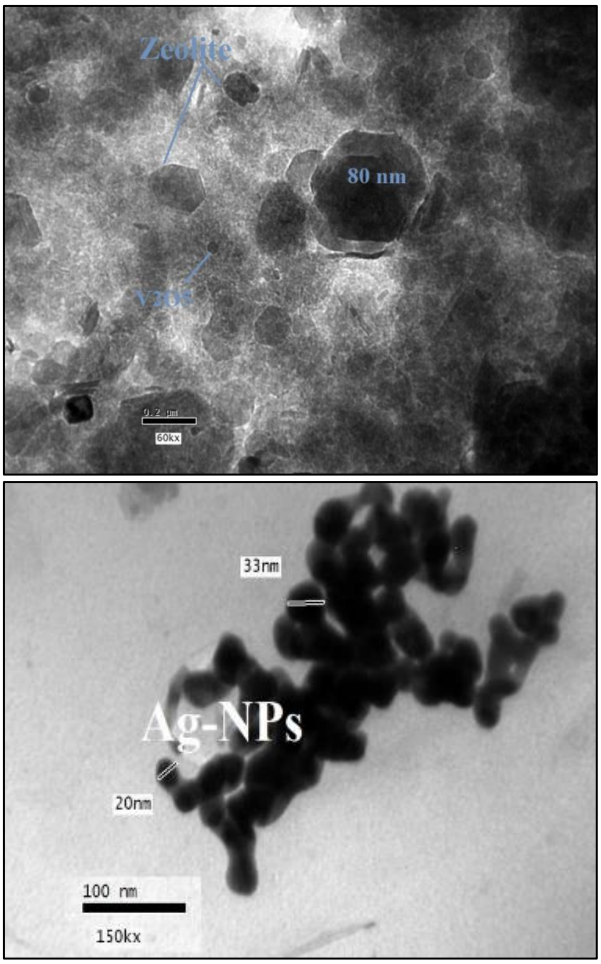

Figure 2: TEM images V_2O_5 / zeolite compound, & Ag-NPs

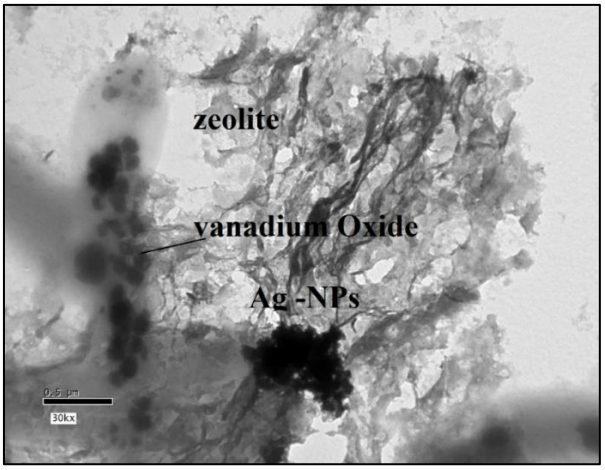

Figure 3: Representative TEM V2O5/ Zeolite /Ag Composite

The TEM image in figure (3) is illustrated the capacity and uniform spread of Vendome oxide, and graphene nanoparticles spread on zeolite surface solution V2O5 has unique morphology dissociation on clay surface our explanation, it could be cations exchange clay cations, and Vendome Metals or return back the electronic configuration of iron: [Ar] $3d^6$ $4s^2$ (ferromagnetism), it is loss e- to be half field d-orbital outer shell with forming chelating complexes with anion (silicate, and aluminate) of zeolite structure. as wall the Nano size structure of Vendome around 15 nm and its crystallographic shape, which is also facilities to make chelating complexes with other compounds .in case graphene assembled on clay. Which has seen in figure (3) various zeolite layers flocculated has appeared on the spread area on the clay surface. Graphene is the main reason for aggregation and depletion of a thin layer of zeolite based on Vander Waals interaction forces between molecules.

3.1.3 XRD characterization

3.1.3.1 XRD zeolite

With regard fig (4), The XRD patterns of zeolite and its additives describe several sharp attribute peaks at 2θ values of 7º, 10.2º, 12.6º, 16.4º,22.6º, 24º, 26.6º, 27.8º, 31º, 31.6º, 31.7º, 32.7º, 33.4º, and 34.5ºis agree with previous literature,37 which was indexed to the (200), (220), (222), (420), (440), (600), (622),(640), (642), (694), (600), (841), (842) and (662) casting back the cubic crystalline structure .as far .there is no big change zeolite /V2O5 samples .which it shows the same pattern, with specific peaks related to vanadium oxides, our explanation, it could back vanadium oxides nanoparticles fill out voids interlayer space, which lead to resulting in the decrease of crystallinity.

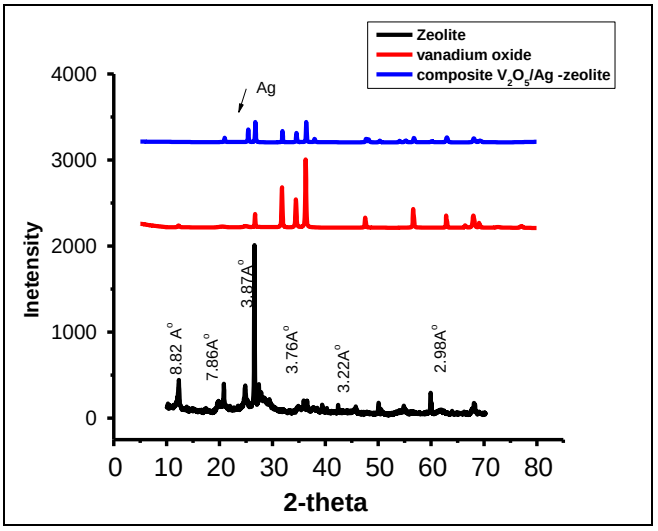

Figure 4: XRD zeolite, vanadium oxide, and composite

The above XRD spectra display that composite of papered catalyst that is composed of a different anionic specious moreover minerals, such as; sodium, silicate, aluminate, and quartz. This mineral has an octahedral crystal structure made of crystallized silica (silicon dioxide, SiO_2), throughout figure (4), we observed several sharp peaks are impurities identical to quartz and silicate. There are some diffraction peaks that appear at (001), (110), (210) plane at 2θ 82, 35, and 66. The X-ray diffraction analysis of vanadium oxides powder (Figure 4) manifests different peaks has been investigated at 2θ (º) = 18.7, 32.1, 34.5, 36.2, 44.2, 55.5, 56.0, 62.6, and 74.6 are allocated to (V_2O_5).

3.1.3.2 Polyethylene high density (PEHD) thermo-gravimetric characterization

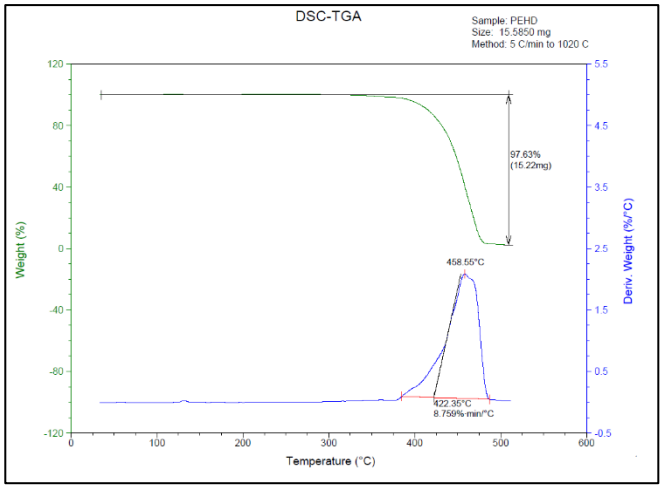

Figure 5: Show DSC –TGA of HDPE

Curve PEHD showed in Figure 5 reveals a decline peak at 458 ⁰C due to changing the solid phase to the liquid phase at glassy temperature. at a certain temperature the large polymeric materials of PEHD start to break down to saturated and unsaturated monomers, hundred of reaction mechanism occurs, leading to forming liquefied gases. The main reason for that measurement, we need to know which best temperature will be completely converted to gases without liquid or waxes. At 458 ⁰C we

noticed, several unsaturated and long-chain hydrocarbon results, thus we applied gasification on PEHD at 600 °C to get rid of all waxes residual. Fig (5) points out the decomposition HDPE at a flow rate of 10 C/min. there are big changes in polyethylene mass fraction around 400 ºC to 520 ºC. As well as release bi-products (CO, CO_2, and H_2O) from the polymeric carbon chain. However, at a certain temperature of 422 °C the polymeric PEHD is lost 8.795 % min/c of its weight.

3.1.4 UV-vis absorption analysis

To evaluate and measure sliver, and vanadium inside papered, we should utilize UV-vis spectra. Samples was performed around 200 to 1000 nm to figure 6 is pointed out, there are three different peaks silver nanoparticles solution, zeolite /vanadium oxide, and their composite sliver nanoparticles appear strong peak at 270 nm, addition to anther peak was appeared specified for vanadium oxide /zeolite compound, which is slightly shifted absorbance peak 297 nm, furthermore, appearing as weak peak. to explain the spectrum shifted, it might be returned, oxidation of v^{+2} to v^{+3}, v^{+5} with zeolite structure (many anion exchanger (SiO3, Al^{+3}, Ca^{+2}, Na, and SiO_2). As far, we notice abroad peak as far specific for the colloidal solution, which contains all specious, might due to creation of active sites between sliver, and vanadium (metallic bond), addition assembled of sliver, vanadium particles on the surface of the zeolite.

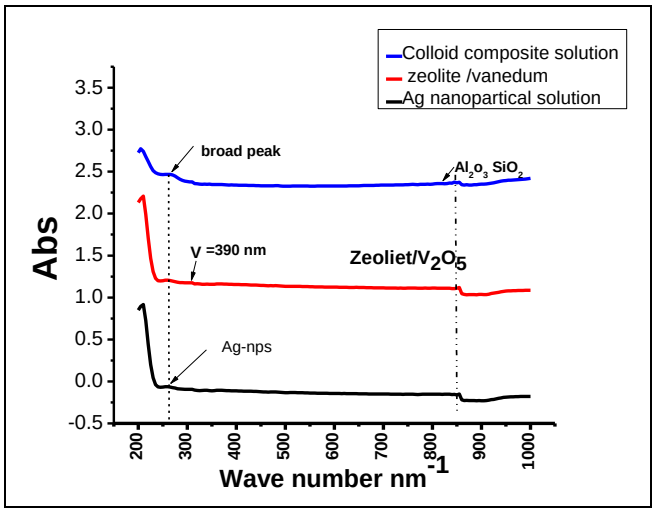

Figure 6: UV-Vis-NIR analysis sliver NPs, zeolite /V2O5, and their composite in colloid solution

The UV–Vis diffuse reflectance characterization in the region (Fig. 6) confirm distinct outcome for the impregnated vanadium samples. From the previous information, the peak intensity is an indicator for the vanadium atoms spectra in this region which are located range 325–500 nm, as well as confirming the transfer of low energy electrons between O and V5+ v outer shall vanadium atoms in octahedral coordination (Gao and Wachs, 2000; Burcham et al., 2000). On the other hand, we noticed a little shift to peaks ranging 270–340 nm is concerning to coordination of the tetrahedral of vanadium. Two peaks are a good indicator for charge transfer resulting from oxidizer V^{2+} to V^{5}+, and reduction of zeolite throughout anionic terminals and oxygen anions.

3.2 Studying the Optimized Parameters of the Degradation Process

Present, zeolite and its modified are mainly utilized in the cracking process of the petrochemical industry. It mostly used as an active adsorbent catalyst for many processes during the purification and decoloration of crude oil. that sorts of hetero- catalysts is working on cracking of heavy fractions, etherification, esterification, alkylation, dehydration, and hydration of hydrocarbon compounds (Yang et al., 2002).

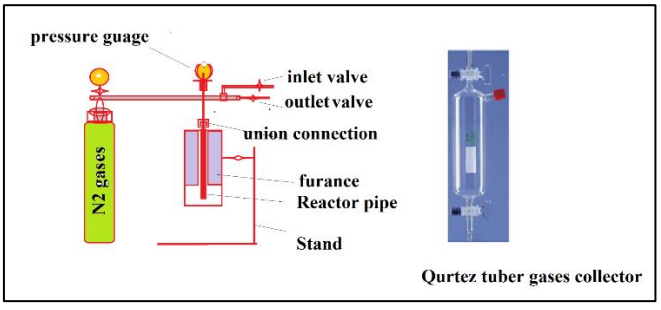

Figure 7: Gasification system

Figure (7) points out the gasification design used for thermos-catalytic degradation of a sample polyethylene high density, it should selective specific parameters to obtain high efficiency of gases and solid waste. There are various factors affecting reaction mechanisms such as temperature, the catalyst used, time of reaction, and pressure. We reported a gradual increase in pressure and temperature during one hour to be stable.

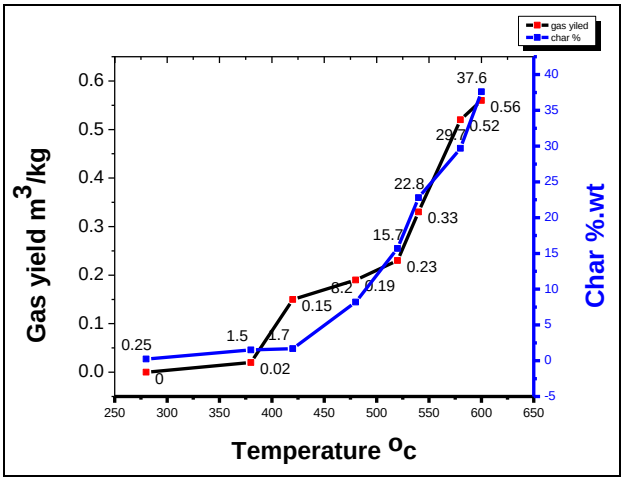

Figure 8: PEHD Gasification in presence Zeolite

Regard figure (8) illustrated the gasification of polyethylene high density using zeolite without modified. There are gradually increase both solid char, and gas yield with increasing temperature gas yield is increases 0.25 to 37.6 m3/kg addition to, char solid also increase to be maximum amount 0.56 at 650 °C. With the highest values of the resulting char solid, there is no good cracking conversion of plastic PE compared to modified zeolite composite at the same reaction conditions (temperature, reaction time).

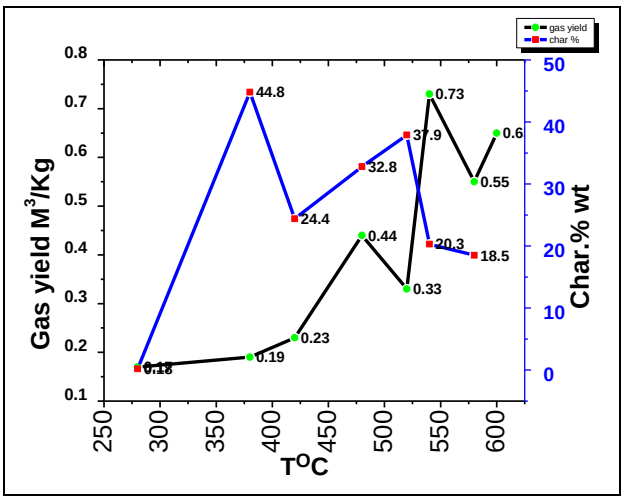

Figure 9: PEHD Gasification in presence Zeolite/V_2O_5/Ag

While using 0.2 g of prepared zeolite /V_2O_5/Ag composite on gasified PEHD sample, we noticed there are big changes in gas yield and char solid. Gas yield is gradually increased from 0.18 to 0.44 at 475 °C then dropped to 0.33 at 525 °C then to return back 0.73 high value of gas yield at 550 °C That is a good indicator for affective of modified zeolite composite on distribution on PEHD surface based on active sides of anionic exchange and electrochemical cell $V^{3+}Ag^{0}$ //$V^{5+}Ag^{-}$ (redox-oxidizing state). On the other hand, solid char is also gradually increased till reaching maximum amount44.8% wt at 350 °C then steadily declined to 18.5 a 575°C. That is results are affirmed on the optimized temperature for gasification polyethylene high-density to gases at 550 °C (high gas yield, and lower solid char) as shown in figure (9)

3.2.1 Gases Yield distribution characterize

Hundreds of organic molecules resulting from the thermal degradation of polyethylene at certain conditions (heating rate, and reaction time) and process parameters (sample, catalyst loading ratio). Gas yield distribution for different cases is shown in fig (10). First, without applied zeolite, Nemours of unsaturated hydrocarbons like alkenes, alkynes, and heterocyclic compounds, addition to High ratio of solids char carbon (CO,

CO_2). But that satiation is comparatively different in case using nature zeolite, with the presence of oxide organic compound like (, benzoic acid, phenolic compounds) results of gasification and there are obviously increasing in gases yield than char carbon. Incase modified catalyst (V_2O_5-Zeoliet-Ag), there are high indications for both quality and quantity of gas yields as well as reducing of heterocyclic, and unsaturated compounds, and increase paraffinic compounds.

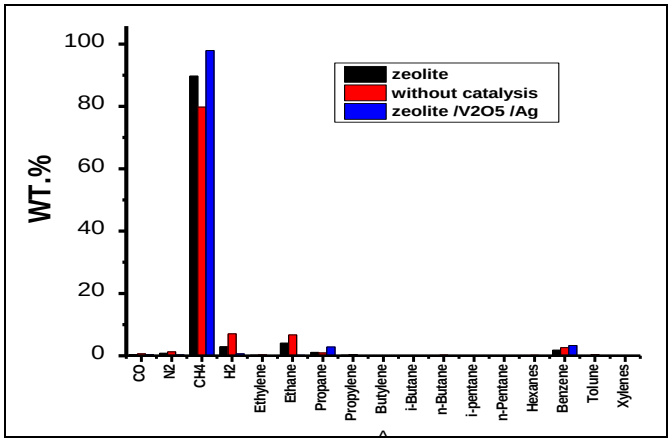

Figure 10: GC analysis for PEHD Gasification in presence Zeolite/V_2O_5/Ag

3.2.2 Solid char characterization

Carbon Char has many industrial applications as raw material or adsorbent materials, catalyst, and incineration. Thus, we reached to convert plastic waste (PE) to gases and solids char, without liquid and waxes at convenient temperature 550^{0}c to 600^{0}c. regarding the TEM image in fig (11), we noticed the brightness of metals in the char sample, which confirms the stability of the prepared catalyst during the gasification process as well as complete conversion for plastic PE.

Figure 11: TEM Gasified PEHD Char sample

3.2.2.1 EDX characterization

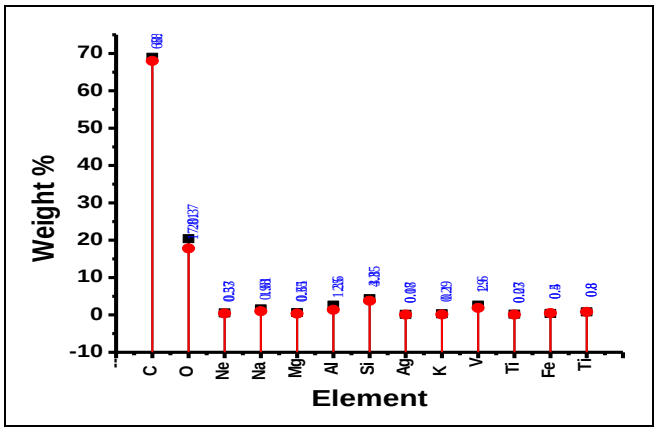

Figure 12: EDX Gasified PEHD Char sample

Furthermore, when applied EDEX on char sample, we found, the sample contains a strain of metals element which are the main content of our composite, like vanadium, Na, silicate, sliver, and carbon. it is a good inductor to integrate element with char which enrich the quality of char as bi-product or raw material reused.

4. Conclusion

The aim of this study was to get active catalyst higher efficiency than nature zeolite, as well as enrich gas yield products, and quality of light hydrocarbon and paraffinic compounds. in that work, we reached to get hetro catalyst works on the degradation of polyethylene high-density to distribution gases without wax (erosion, pipes blocked) and liquid compounds event at 550 ^{o}C for 45 minutes. Furthermore, high conversion of plastic to lower amount of solids char (easily remove from the fixed reactor, and be applicable to another field) Catalyst is composed of vanadium oxide, Nanosilver, and zeolite substrate not only highly ratio of gases yields distribution, but also the quality of gas products like syngas, Hydrogen, and paraffinic compounds. The conjunction between metals alloy (vanadium, and sliver) on zeolite anion exchange cross-section is the main reason for reducing active energy, to complete conversion for PE at 550°C. The deposition, and assembly of vanadium oxides and sliver on zeolites layer sheets enhance the activity of zeolite catalyst regard to previous results and measurements. That integration is also created several active sites on the zeolite surface, which lead to forming a chelating complex during transition phase temperature, then created several of saturated hydrocarbon and paraffinic light compounds.

References

Abdelrahman, A., Radwan, A.M., Zaki, A.H., Hamouda, A.S. 2021. Assembling a Bunch of Transition Metals Oxides on Sodium Montmorillonite Layer for Anionic Polymerization of Butyl Methyl Acrylate. Journal of Nanostructures, 11(1), pp. 1-12.

Akah, A. 2017. Application of rare earths in fluid catalytic cracking: A review. Journal of Rare Earths, 35(10), pp. 941-956.

Albrecht, T.A., Stern, C.L., Poeppelmeier, K.R. 2007. The Ag2O– V2O5– HF (aq) System and Crystal Structure of α-Ag3VO4. Inorganic chemistry, 46(5), pp. 1704-1708.

Bertau, M., Offermanns, H., Plass, L., Schmidt, F., Wernicke, H.J. eds. 2014. Methanol: the basic chemical and energy feedstock of the future, pp. 677. Heidelberg: Springer.

Burcham, L.J., Deo, G., Gao, X., Wachs, I.E., 2000. In situ IR, Raman, and UV-Vis DRS spectroscopy of supported vanadium oxide catalysts during methanol oxidation. Topics in Catalysis, 11(1-4), pp. 85-100.

De Klerk, A. 2007. Environmentally friendly refining: Fischer–Tropsch versus crude oil. Green Chemistry, 9(6), pp. 560-565.

de Klerk, A. 2008. Fischer–Tropsch refining: technology selection to match molecules. Green Chemistry, 10(12), pp. 1249-1279.

Gao, X., Wachs, I.E., 2000. Investigation of surface structures of supported vanadium oxide catalysts by UV– vis– NIR diffuse reflectance spectroscopy. The Journal of Physical Chemistry B, 104(6), pp. 1261-1268.

Hagiwara, K., Ebihara, T., Urasato, N., Ozawa, S., Nakata, S., 2003. Effect of vanadium on USY zeolite destruction in the presence of sodium ions and steam—studies by solid-state NMR. Applied Catalysis A: General, 249(2), pp. 213-228.

Hu, Z., Jiang, E., Ma, X. 2019. The effect of oxygen carrier content and temperature on chemical looping gasification of microalgae for syngas production. Journal of the Energy Institute, 92(3), pp. 474-487.

Hu, Z., Ma, X., Chen, C. 2012. A study on experimental characteristic of microwave-assisted pyrolysis of microalgae. Bioresource technology, 107, pp. 487-493.

Jeon, H.J., Park, S.K. and Woo, S.I. 2006. Evaluation of vanadium traps occluded in resid fluidized catalytic cracking (RFCC) catalyst for high gasoline yield. Applied Catalysis A: General, 306, pp. 1-7.

Jones, R.L. 1991. Oxide acid-base reactions relating to the inhibition of vanadium attack on REY zeolite catalysts. Journal of Catalysis, 129(1), pp. 269-274.

Konta, R., Kato, H., Kobayashi, H., Kudo, A. 2003. Photophysical properties and photocatalytic activities under visible light irradiation of silver vanadates. Physical Chemistry Chemical Physics, 5(14), pp. 3061-3065.

Kostyniuk, A., Bajec, D., Likozar, B. 2021. Catalytic hydrogenation, hydrocracking and isomerization reactions of biomass tar model compound mixture over Ni-modified zeolite catalysts in packed bed reactor. Renewable Energy, 167, pp. 409-424.

Liang, J., Shan, G., Sun, Y. 2021. Catalytic fast pyrolysis of lignocellulosic biomass: Critical role of zeolite catalysts. Renewable and Sustainable Energy Reviews, 139, pp. 110707.

Maitlis, P.M., de Klerk, A. eds. 2013. Greener Fischer-Tropsch Processes: For Fuels and Feedstocks. John Wiley & Sons.

Pine, L.A. 1990. Vanadium-catalyzed destruction of USY zeolites. Journal of Catalysis, 125(2), pp. 514-524.

Possato, L.G., Diniz, R.N., Garetto, T., Pulcinelli, S.H., Santilli, C.V., Martins, L. 2013. A comparative study of glycerol dehydration catalyzed by micro/mesoporous MFI zeolites. Journal of catalysis, 300, pp. 102-112.

Rapagnà, S., Jand, N., Kiennemann, A., Foscolo, P.U. 2000. Steam-gasification of biomass in a fluidised-bed of olivine particles. Biomass and bioenergy, 19(3), pp. 187-197.

Saad, J.M., Williams, P.T. 2017. Pyrolysis-catalytic dry (CO2) reforming of waste plastics for syngas production: Influence of process parameters. Fuel, 193, pp. 7-14.

Sun, Z., Luo, S., Qi, P., Fan, L.S. 2012. Ionic diffusion through Calcite (CaCO3) layer during the reaction of CaO and CO2. Chemical Engineering Science, 81, pp. 164-168.

Swabb, E.A., Gates, B.C. 1972. Diffusion, reaction, and fouling in H-mordenite crystallites. The catalytic dehydration of methanol. Industrial & Engineering Chemistry Fundamentals, 11(4), pp. 540-545.

Verboekend, D., Mitchell, S., Milina, M., Groen, J.C., Pérez-Ramírez, J., 2011. Full compositional flexibility in the preparation of mesoporous MFI zeolites by desilication. The Journal of Physical Chemistry C, 115(29), pp. 14193-14203.

Verboekend, D., Pérez-Ramírez, J. 2011. Design of hierarchical zeolite catalysts by desilication. Catalysis Science & Technology, 1(6), pp. 879-890.

Wallenstein, D., Schäfer, K., Harding, R.H., 2015. Impact of rare earth concentration and matrix modification in FCC catalysts on their catalytic performance in a wide array of operational parameters. Applied Catalysis A: General, 502, pp. 27-41.

Wormsbecher, R.F., Peters, A.W., Maselli, J.M., 1986. Vanadium poisoning of cracking catalysts: mechanism of poisoning and design of vanadium tolerant catalyst system. Journal of Catalysis, 100(1), pp. 130-137.

Xu, M., Liu, X., Madon, R.J. 2002. Pathways for Y zeolite destruction: The role of sodium and vanadium. Journal of Catalysis, 207(2), pp. 237-246.

Yang, H., Wilson, M., Fairbridge, C., Ring, Z., Hill, J.M., 2002. Mild hydrocracking of synthetic crude gas oil over Pt supported on pillared and delaminated clays. Energy & fuels, 16(4), pp. 855-863.

Yao, D., Wu, C., Yang, H., Zhang, Y., Nahil, M.A., Chen, Y., Williams, P.T., Chen, H. 2017. Co-production of hydrogen and carbon nanotubes from catalytic pyrolysis of waste plastics on Ni-Fe bimetallic catalyst. Energy Conversion and Management, 148, pp. 692-700.